Journal of Applied Geophysics 250 (2026) 106266

Contents lists available at ScienceDirect

Journal of Applied Geophysics

journal homepage: www.elsevier.com/locate/jappgeo

Spectral decomposition reveals Hidden Fluvial channels: Implications for geothermal potential in the Karlsruhe Area, Upper Rhine Graben, Germany

Amr Talaat Tolba *, Florian Bauer, Jens Carsten Grimmer, Ali Dashti, Thomas Kohl

Karlsruhe Institute of Technology (KIT), Karlsruhe, Germany

ARTICLE INFO

Keywords:
Thermal storage
Middle-deep geothermal utilization
Upper Rhine Graben
Spectral decomposition
Fluvial channels
Oligocene

ABSTRACT

This study employed advanced seismic analysis techniques to enhance our understanding of subsurface geology for geothermal utilization. Focusing on a rectangular 10 km × 4 km area encompassing the Campus North of the Karlsruhe Institute of Technology (KIT) and including the former Leopoldshafen oil field, we investigated the ca. 250 ± 25 m thick late Oligocene (Chattian) Niederrödern Formation to analyze the geometries of up to 15 m thick sand layers. The initial interpretation of a pre-stack depth-migrated (PSDM) seismic cube using conventional attributes failed to resolve these small-scale features. To overcome these limitations, we implemented spectral decomposition techniques that convert seismic signals into their constituent frequencies using a short-time Fourier transform (STFT) algorithm. The applied spectral decomposition covered a frequency range of 10–60 Hz, with optimal imaging achieved at 10, 26, and 40 Hz. A total of 25 fluvial channels were identified within the Late Oligocene interval at depths between 178 and 1155 m. Individual channels exhibit widths of approximately 25–100 m and spectrally derived thicknesses of 15–24 m, which were previously unrecognized using conventional seismic interpretation techniques, spectral decomposition improved lateral channel detectability by more than one tuning thickness, enabling the resolution of features below the nominal seismic vertical resolution. Particular emphasis is placed on analyzing the geometry and dimensions of these channels to enable more specific thermo-hydraulic (TH) modeling and assess their suitability and boundary conditions for thermal storage. The fluvial channels appear to be stacked within the generally >200 m thick stratigraphic succession, distributed across the stratigraphic record and the three tectonic blocks. In our small survey, the apparent decrease in sinuosity with time may reflect an increase in stream power over time, possibly due to the initiation of subsidence in the Heidelberg Basin, which is the most distinct late Oligocene-Neogene depocenter in the northern URG.

1. Introduction

The global transition toward sustainable energy sources has intensified the exploration and development of geothermal resources as a reliable, baseload renewable energy option. Geothermal energy, derived from the Earth's internal heat, offers significant advantages over intermittent renewable sources due to its consistent availability and minimal environmental footprint (Ogola et al., 2012).In Central Europe, the Upper Rhine Graben (URG) has emerged as a region of exceptional geothermal potential, characterized by elevated heat flow and complex geological structures that facilitate heat transport to economically viable depths.

The Karlsruhe area, situated in the northern section of the URG in Germany, represents an auspicious location for geothermal exploration and development. This region exhibits subsurface temperatures of up to 140 °C at a relatively shallow depth of 2 km, making it an ideal candidate for both direct heat utilization and electricity generation (Agemar et al., 2012). These favorable thermal conditions are primarily driven by two key factors: elevated regional heat flow resulting from crustal thinning and localized thermal anomalies associated with fault-controlled fluid circulation systems (Pribnow and Schellschmidt, 2000).

Despite the recognized geothermal potential of the Karlsruhe area, detailed characterization of subsurface structures remains challenging. Conventional seismic interpretation methods often fail to resolve smaller-scale features that may significantly influence fluid flow pathways and heat transport mechanisms. Of particular interest are the fluvial channel systems deposited during the Oligocene epoch, which could serve as preferential fluid conduits within the broader

* Corresponding author.
E-mail address: amr.talaat@kit.edu (A.T. Tolba).

https://doi.org/10.1016/j.jappgeo.2026.106266
Received 3 December 2025; Received in revised form 23 February 2026; Accepted 10 April 2026
Available online 12 April 2026

sedimentary sequence. These channels formed approximately 33.9 to 23 million years ago, represent a critical component of the complex depositional history that shaped the current subsurface architecture of the URG.

This study investigates a 10 km × 4 km rectangular area surrounding KIT Campus North, focusing on the approximately 250 ± 25 m thick Niederrödern Formation. The primary aim is to enhance subsurface imaging to delineate sand layers, some as thin as 15 m, which are critical for assessing the formation's geothermal potential. Traditional seismic attributes derived from pre-stack depth-migrated (PSDM) seismic data have been limited in resolving these fine-scale features (Marfurt and Alves, 2015). To overcome these constraints, we employ spectral decomposition techniques, utilizing a short-time Fourier transform (STFT) algorithm to decompose seismic signals into their constituent frequency components (Partyka et al., 1999). By integrating RGB-blended spectral decomposition displays, as described by (Marfurt and Alves, 2015), we aim to identify previously unrecognized geological structures, such as narrow fluvial channels, and analyze their geometry and distribution. These findings are essential for informing thermo-hydraulic (TH) modeling and evaluating the suitability of the formation for thermal storage applications (Kolditz et al., 2012).

The identification of meandering fluvial channels, some as narrow as 25 m, provides new insights into the complex depositional history of the Niederrödern Formation. These channels, distributed across three tectonic blocks within the study area, reflect the interplay of sedimentary and tectonic processes in the northern URG (Derer et al., 2005). Sandstones in continental rift basins are important reservoirs for fluids. Independent of their diverse origins (fluviatile, lacustrine, marine, or eolian), depth, thickness, and geometry, as well as petrophysical properties, are important parameters for utilizing sandstone for thermal storage (e.g., Stricker et al., 2020). Geometry and thickness are also important for drill path planning, TH-modeling, reservoir development, and management. The identification of sandstone layers and lenses with thicknesses <20 m in seismic surveys is challenging and commonly documented only by borehole data. Therefore, we applied advanced seismic analytical tools to identify thin sandstone bodies within a marly-mudstone matrix and their geometries in a 250 ± 25 m thick sedimentary *syn*-rift sequence, comprising the late Oligocene fluvial-lacustrine succession of the Niederrödern Formation in the central segment of the Upper Rhine Graben.

Recent advances in spectral and physics-based modeling approaches have substantially improved the characterization of geothermal systems and sedimentary heterogeneities at multiple scales. For instance, (Naseer, 2026) demonstrated that spectral decomposition integrated with temperature and water-saturation–constrained dynamic simulations can effectively delineate high-temperature geothermal resources, highlighting the value of frequency-dependent seismic attributes for reservoir discrimination and thermal assessment. Complementarily, (Zhao et al., 2024) employed multi-scale numerical simulations to quantify preferential flow pathways in heterogeneous soils, underscoring the importance of dimensionality and scale when interpreting subsurface flow architectures. Further illustrate the capability of frequency-based analyses to resolve mineralogical and lithological variability, while momentum-based sediment flux modeling in fluvial systems (Zhang et al., 2025) provides process-oriented constraints on channel geometry and stacking patterns. Building upon these global developments, the present study applies RGB-blended spectral decomposition to image thin fluvial channel systems within the Upper Rhine Graben and translates frequency-domain attributes into geometrical and thickness estimates relevant for geothermal reservoir assessment. In doing so, this work bridges spectral imaging, sedimentary process understanding, and geothermal reservoir evaluation within a unified methodological framework.

Furthermore, the application of advanced seismic analysis techniques underscores their value in unlocking the potential of geologically complex formations for sustainable energy applications (Brown, 2011; Lala and Talaat, 2020; Marfurt and Alves, 2015).

2. Regional geology of the Upper Rhine Graben

The c. 300 km long and 30–40 km wide URG is part of the European Cenozoic Rift System (ECRIS), which extends for about 1000 km from the North Sea to the Mediterranean Sea (Fig. 1),), is bound to the N and S by accommodation zones that separate the URG from the Rhenish Massif and the Lower Rhine Graben in the NW and the Bresse-Rhone Graben in the SW (Fig. 1). The URG is internally subdivided into southern, central, and northern segments by accommodation zones (Grimmer et al., 2017). The accumulated Cenozoic sediments, including up to 350 m of Quaternary successions, comprise an up to 3500 m thick, predominantly low-energy sedimentary succession in the URG (Geyer et al., 2011). The estimated total extension in the URG is 7–18% (Grimmer et al., 2017). As is typical for narrow, non-magmatic rifts with less than 21% total extension, the normal fault segments in the URG are predominantly linked by relay ramps rather than by transfer faults (Acocella, 2005).

The development of the URG succeeded a phase of Late Cretaceous and Eocene dynamic topography and associated minor volcanism in the Southern Central European Volcanic Province (Binder et al., 2023). The Late Cretaceous to Eocene uplift caused the erosion of large parts of the Mesozoic successions of the subcrop of the northern URG area (Böcker et al., 2017a; Von Eynatten et al., 2021). The early Eocene-Oligocene successions were deposited during a regional WNW extension and the formation of major NE- to NNE-trending depocenters in the southern and central segments (e.g., the Strasbourg-Rastatt Basin; Fig. 1). Stress field change at c. 27 ± 1 Ma superposed N-S to NNW-SSE-trending intra-rift basins (Bauer et al., 2025). In SW Germany and adjacent NE France, subordinate primitive alkaline volcanism occurred between approximately 27 and 9 Ma, possibly linked to stress field changes (Binder et al., 2023). Major volcanic activity in the URG occurred between approximately 18 and 14 Ma in the southern URG (Kaiserstuhl) and northern URG (Vogelsberg; Fig. 1), accompanied by a phase of dynamic topography and an uplift of c. 1000 m in the southern URG (Vosges-Black Forest dome; (Binder et al., 2023; Grimmer et al., 2017). Miocene uplift led to the partial erosion of earlier rift-filling sedimentary sequences in the southern and central segments and to a generally well-documented angular unconformity at the base of the Pliocene-Quaternary strata (e.g., Geyer et al., 2011). This rift-wide unconformity is overlain by variable Pliocene to Holocene fluvial and (minor) eolian sediments, which generally plunge NNE-ward in the study area. Post-Miocene sediments were probably deposited during cooling-induced subsidence, which followed a phase of Miocene dynamic topography (Binder et al., 2023).

The stratigraphy of the central URG is displayed in Fig. 2, and the seismic characterization of the seismic horizons is described by (Bauer et al., 2025). Eocene to Oligocene fluvio-lacustrine to brackish-marine sedimentary sequences form the main early *syn*-rift sequences, the Haguenau and Pechelbronn Formations (Fm.), and occur in all segments of the URG, with the southern and central segments forming major depocenters (Berger et al., 2005; Derer et al., 2005). The Haguenau Formation consists of lacustrine clays and marls intercalated with evaporites. The clastic material of the Pechelbronn Fm. originates mainly from the northern part of the URG in the area of the present-day Mainz marginal basin block (Fig. 1). The peak of flooding and associated deposition of marine sediments in the URG occurred during the Rupelian transgression. This resulted in the c. 20–45 m thick Foraminifera marls, overlain by the up to 20 m thick Fish Shale ("Rupel clay"). This "Rupel Clay" forms the basal units of the Froidefontaine Formation and is the most important basin-wide seismic reflector in the URG (for example, Rotstein et al., 2005). The Froidefontaine Fm. (or Grey Bed Series, e.g., Wirth, 1962) consists of uniform, mica-bearing grey marls and centimeter-to several meter-thick sand layers (Geyer et al., 2011). The Froidefontaine Fm. comprises two Rupelian transgression cycles imposing the deposition of several sand layers and lenses, intercalated in a generally marl-dominated succession, and comprising targets for

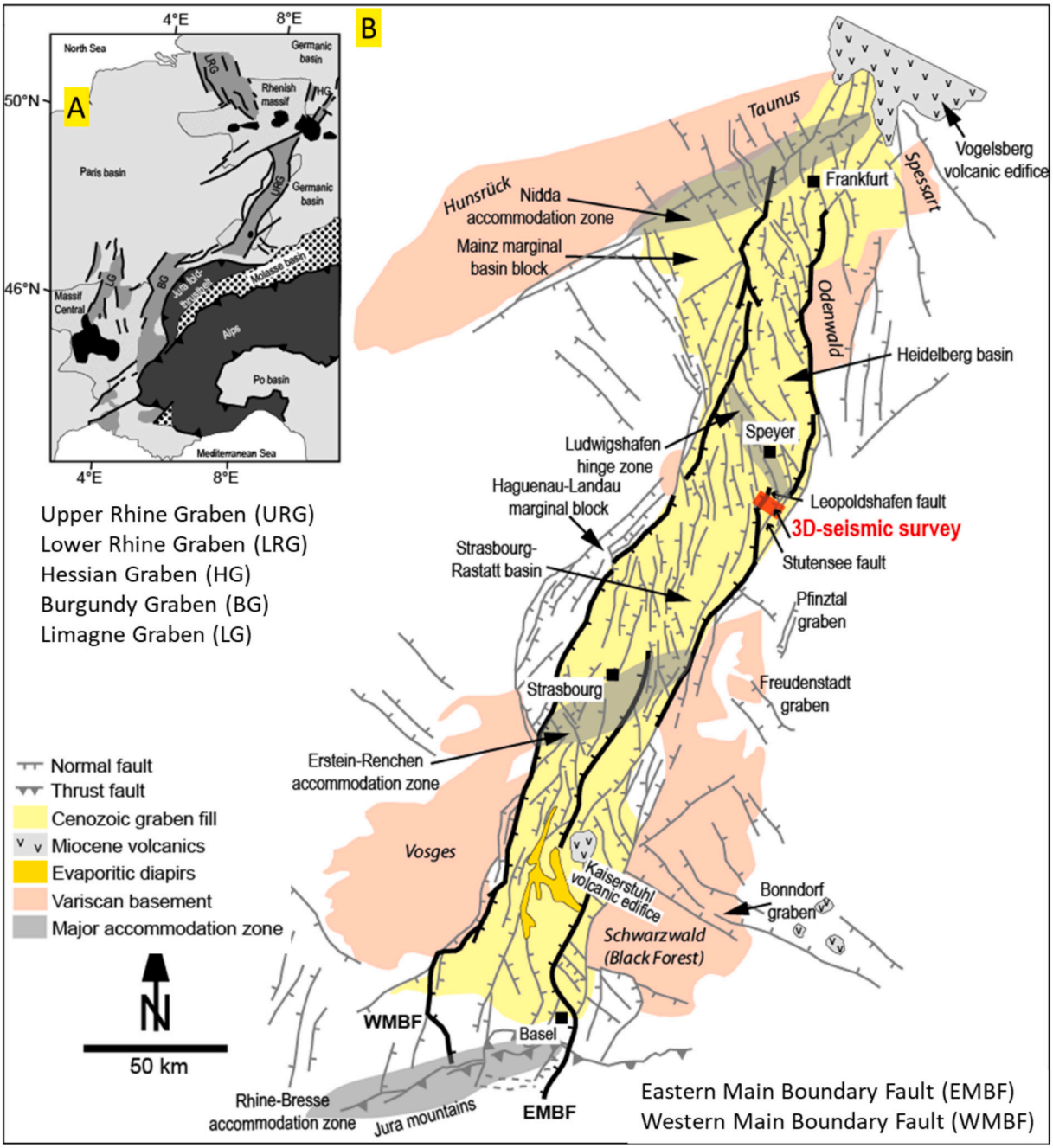

Fig. 1. A) The inset map illustrates the Upper Rhine Graben as a component of the European Cenozoic Rift System (ECRIS), highlighting the principal grabens within this region. The black units denote significant Cenozoic volcanic formations. B) The overview presents the primary structural units of the URG, as adapted from (Grimmer et al., 2017), and indicates the location of the 3D-seismic survey conducted in this study, as well as the Stutensee and Leopoldshafen faults (Bauer et al., 2025).

hydrocarbon exploration and exploitation (Böcker et al., 2017b; Pirkenseer et al., 2013; Reinhold et al., 2016). The subsequent Chattian regression marks the transition from marine (Meletta beds) to brackish (Cyrena marl) to fluviatile deposits of fine-grained siliciclastics and marls of the uppermost Oligocene Niederrödern Fm., deposited unconformably on top of the Froidefontaine Fm. (Bauer et al., 2025). The Niederrödern Fm. is poorly exposed along the graben boundaries and is mostly documented from boreholes. The presence of sand layers and lenses in this stratigraphic unit locally accumulated hydrocarbons (for example, Böcker et al., 2017b). Microfossils indicate freshwater fauna and the deposition of lacustrine-fluviatile sediments (for example, Grimm, 2011). The Oligocene-Miocene boundary at c. 23 Ma lies within the Bruchsal Fm., comprising carbonates with minor sand layers (Cerithia beds) and uniform thin layers of alternating light limestone laminae and dark grey marls with locally significant evaporite accumulations (Corbicula beds; Geyer et al., 2011). The Landau Fm. comprises brackish-marine, early Miocene (Aquitanian-Burdigalian) dolomite-shale interlayers of the Lower and Upper Hydrobia beds, deposited during the Burdigalian transgression at approximately 18–20 Ma (Grimm, 2011; Geyer et al., 2011). The weakly to unconsolidated Pliocene to Quaternary fluvio-lacustrine silt-sand-gravel successions are usually summarized as a single unit in seismic studies and hence are stratigraphically not further differentiated here.

The study area includes the former Leopoldshafen oil field, where 18

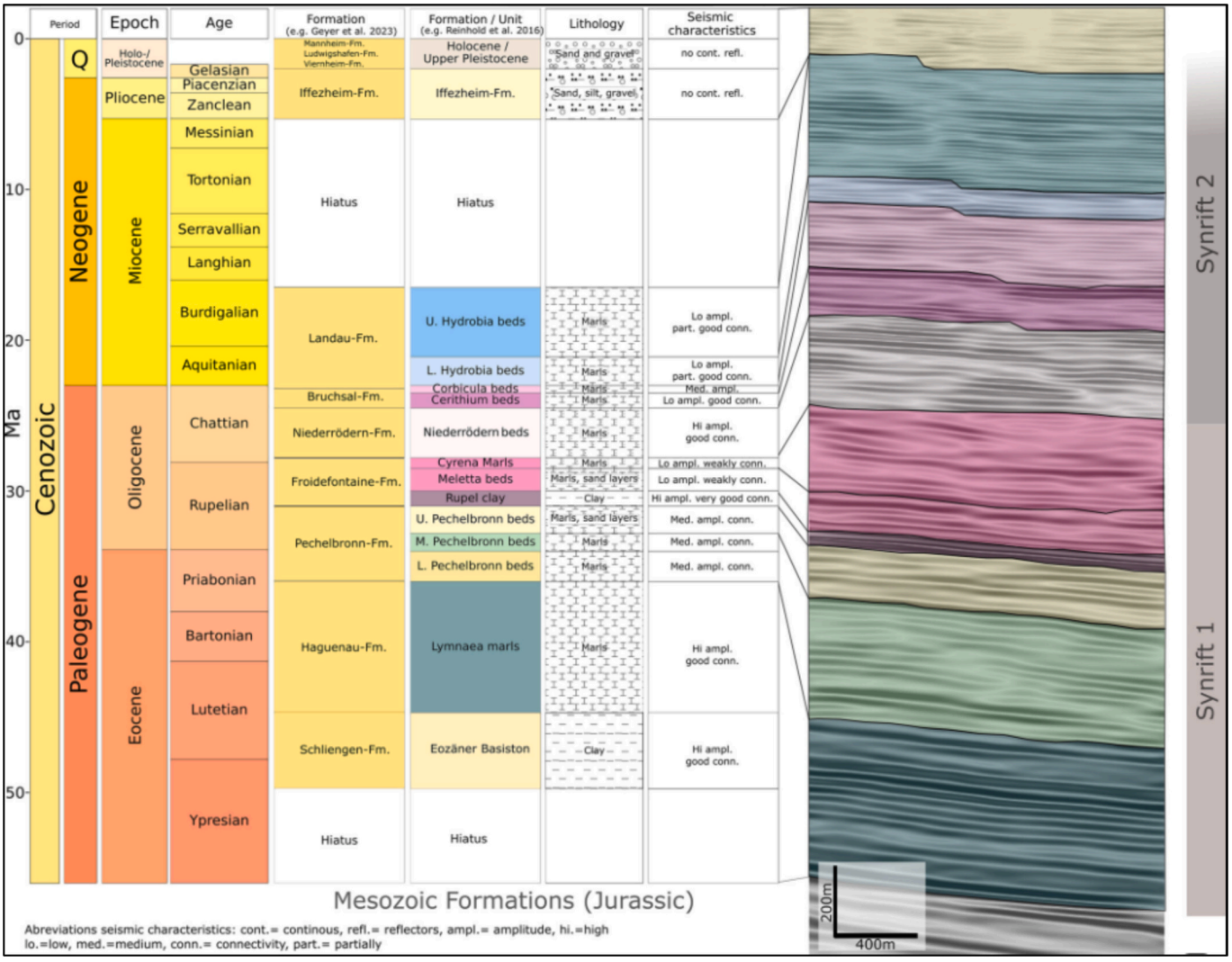

Fig. 2. illustrates the stratigraphic framework, lithological features, and seismic characteristics of the Neogene and Paleogene sedimentary sequences within the study area. The transition from Syn-rift I to Syn-rift II deposits reflects a notable change in the regional tectonic stress regime, as elaborated in the main text. The stratigraphic interpretations are based on the works of (Bauer et al., 2025; Geyer et al., 2011; Reinhold et al., 2016).

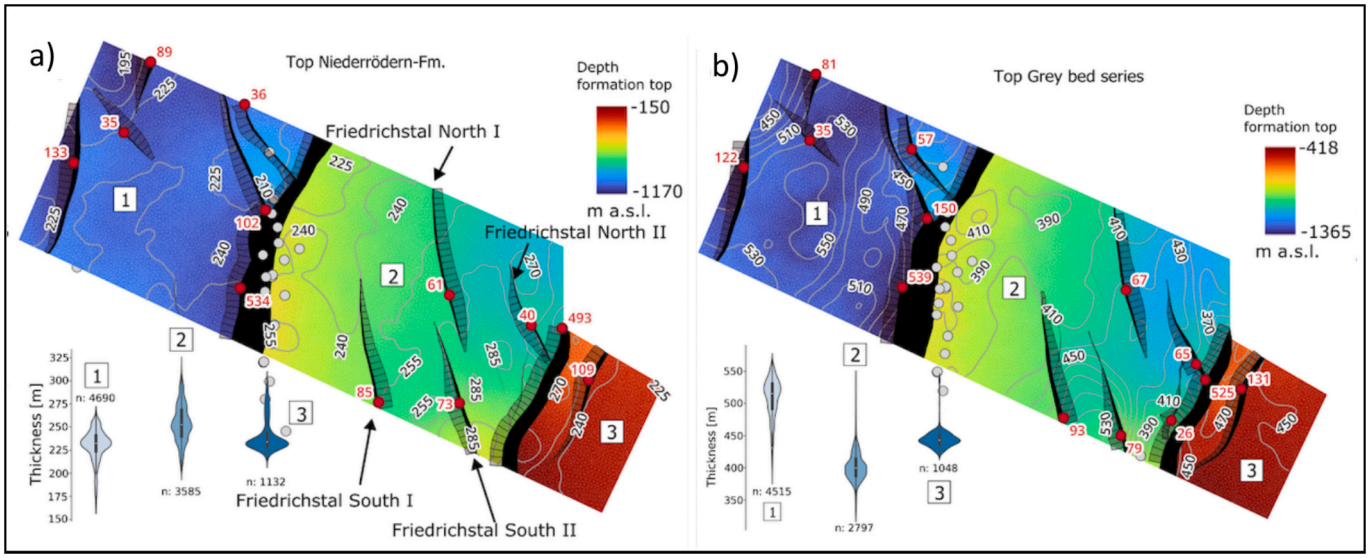

Fig. 3. Formation top maps of a) the Niederrödern Fm. and b) the Froidefontaine Fm. (or Grey bed series) (Bauer et al., 2025).

wells (excluding side tracks) were drilled <2 km into Cenozoic successions from 1956 to 1982. Additional in-field and off-site wells provide further information. Oil was produced from a stacked reservoir in the footwall of the Leopoldshafen fault, including shallow eastward-dipping sandstones of the Meletta Beds, Cyrena marls, and Niederrödern Fm. (Fig. 2). Notably, the majority of wells in the former Leopoldshafen oil field did not intersect the Niederrödern Fm. completely, as parts of the succession were faulted out along the major, deep-rooted NNW-SSE-trending Leopoldshafen normal fault (Fig. 3). Thickness estimates thus rely on a few boreholes, not affected by faulting at the level of the Niederrödern Fm., but mainly on seismic data (Bauer et al., 2025).

3. Materials and methods

3.1. Data availability

This study employed a subset of a high-resolution 3D seismic survey acquired in 2012, encompassing a rectangular area of approximately 10 km × 4 km. The survey area is situated around Campus North of the Karlsruhe Institute of Technology (KIT), including the former Leopoldshafen oil field (Fig. 4). The seismic dataset was processed for pre-stack depth migration (PSDM), enabling optimal imaging of subsurface structures and stratigraphic features. The data offer a vertical resolution of approximately 20 m within the target interval, facilitating a detailed analysis of the Chattian–Oligocene stratigraphy, which occurs between 178 m and 1155 m depth below the surface.

Overall, the quality of the seismic data is classified as good to excellent for the Cenozoic successions across the survey area, although localized degradation is observed in the footwall of major fault zones due to complex wave propagation effects, such as shadowing. The central part of the survey area is characterized by a particularly high signal-to-noise ratio, providing favorable conditions for the application of advanced seismic attribute analysis.

3.2. Conventional seismic interpretation

The initial interpretation of the dataset followed standard workflows, beginning with the identification and mapping of key stratigraphic horizons and structural elements (Bauer et al., 2025). The Late Oligocene sequence was delineated based on characteristic seismic reflection patterns and correlation with regional stratigraphic frameworks established in previous studies of the URG (Derer et al., 2005).

The structural framework of the study area was defined through detailed mapping of major fault systems, with particular emphasis on the NNE-SSW-trending Leopoldshafen and Stutensee faults, which segment the region into three distinct blocks: east, central, and west. Fault interpretation was conducted on a series of inline and crossline sections (Lala and Talaat, 2020) by using OpendTect software, with subsequent 3D visualization to ensure geometric consistency and to identify potential fault interactions that might influence fluid flow pathways. In Fig. 5, a NW-SE seismic line illustrates the Late Oligocene stratigraphy (highlighted in light blue), ranging from 178 to 1155 m subsurface. This figure also delineates the main structural framework, identifying two major NNE-SSW-trending faults, the Leopoldshafen and Stutensee faults, which divide the study area into three blocks: East, Central, and West.

Following the establishment of the structural framework, conventional seismic attribute extraction was performed to enhance the visualization of stratigraphic features (El Kady et al., 2024) within the Late Oligocene interval. In Fig. 6, using Hampson-Russell, root-mean-square (RMS) amplitude maps were generated, which successfully revealed broad stratigraphic layering and gross depositional trends. However, the RMS attribute lacked the resolution required to delineate finer-scale geometries such as channel systems. Even when the Late Oligocene interval was subdivided into multiple sub-zones and attributes were extracted separately for each zone, this strategy did not enhance channel detectability. These limitations underscore the inadequacy of conventional RMS amplitude analysis alone for identifying subtle stratigraphic heterogeneities in complex depositional settings.

Despite the application of these conventional attributes, smaller-

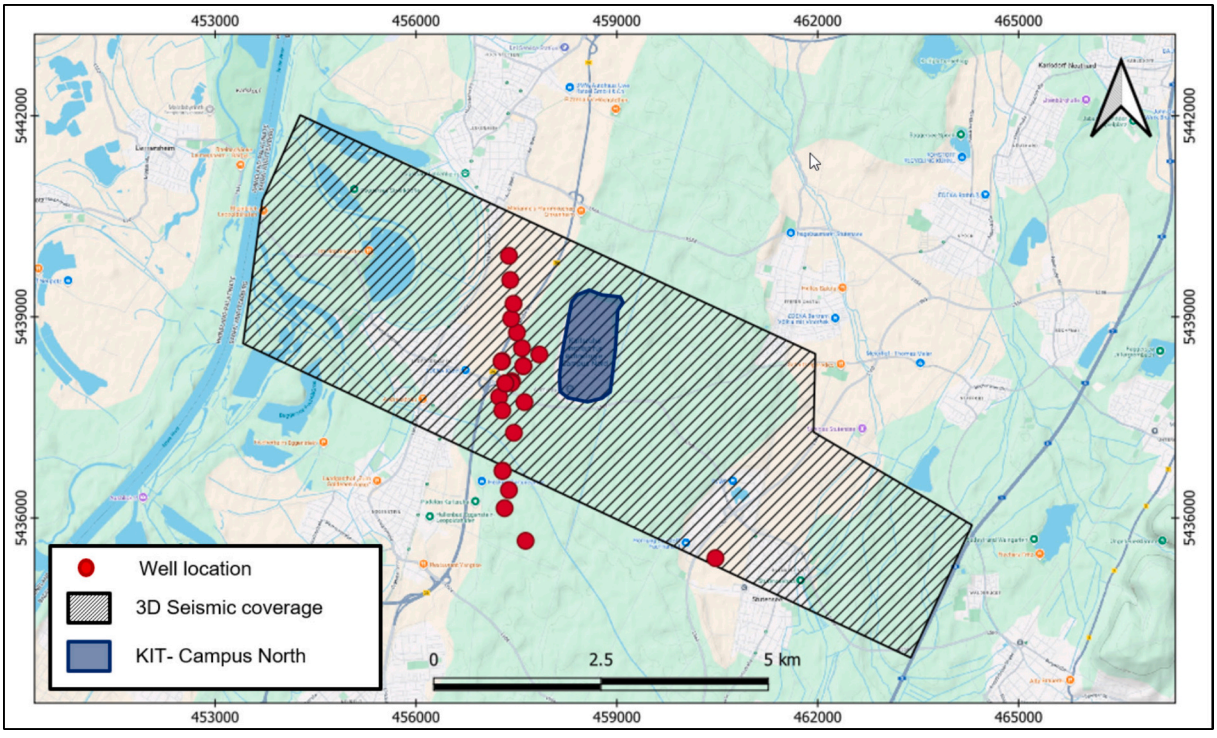

Fig. 4. Base map illustrating the outline of the seismic survey area and KIT Campus North location with wells distribution across the study region.

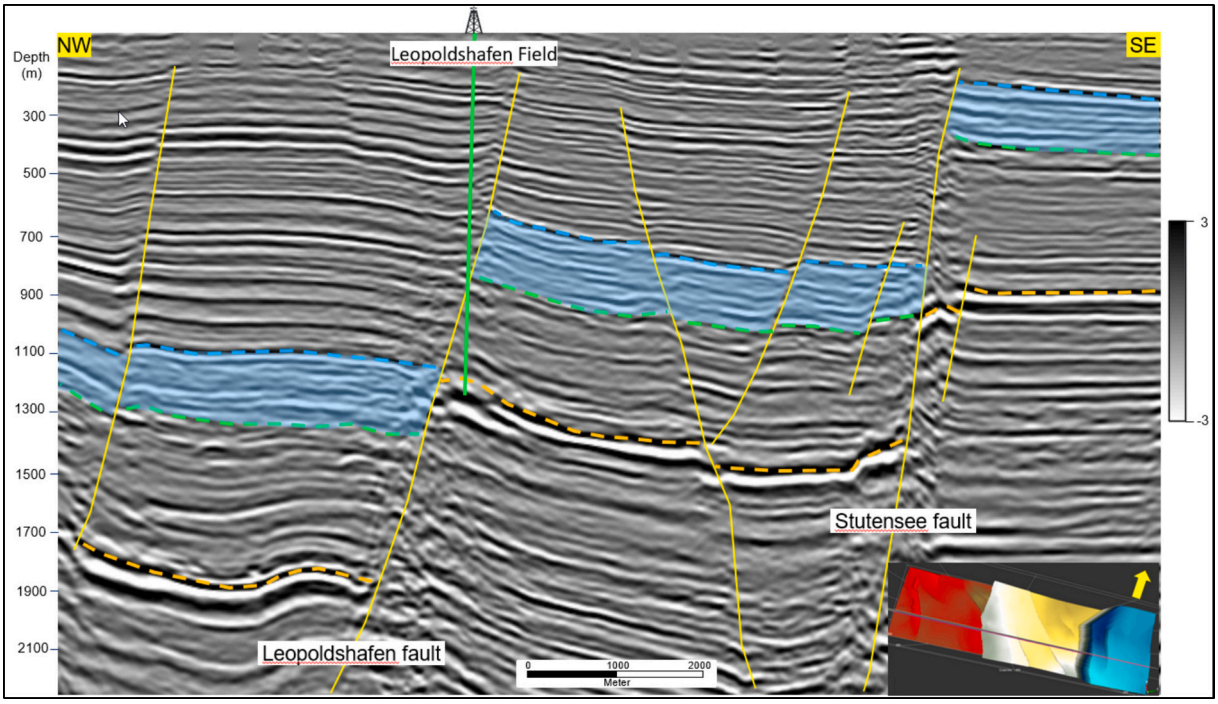

Fig. 5. NW–SE-oriented seismic profile illustrating the principal structural elements within the study area. The zone of interest is delineated by the shaded blue polygon, while the dashed orange horizon marks the Fish Shale unit situated at the base of the Meletta Beds. An example of the well path illustrates the effect of faulting out of the Niederrödern Fm. (For interpretation of the references to colour in this figure legend, the reader is referred to the web version of this article.)

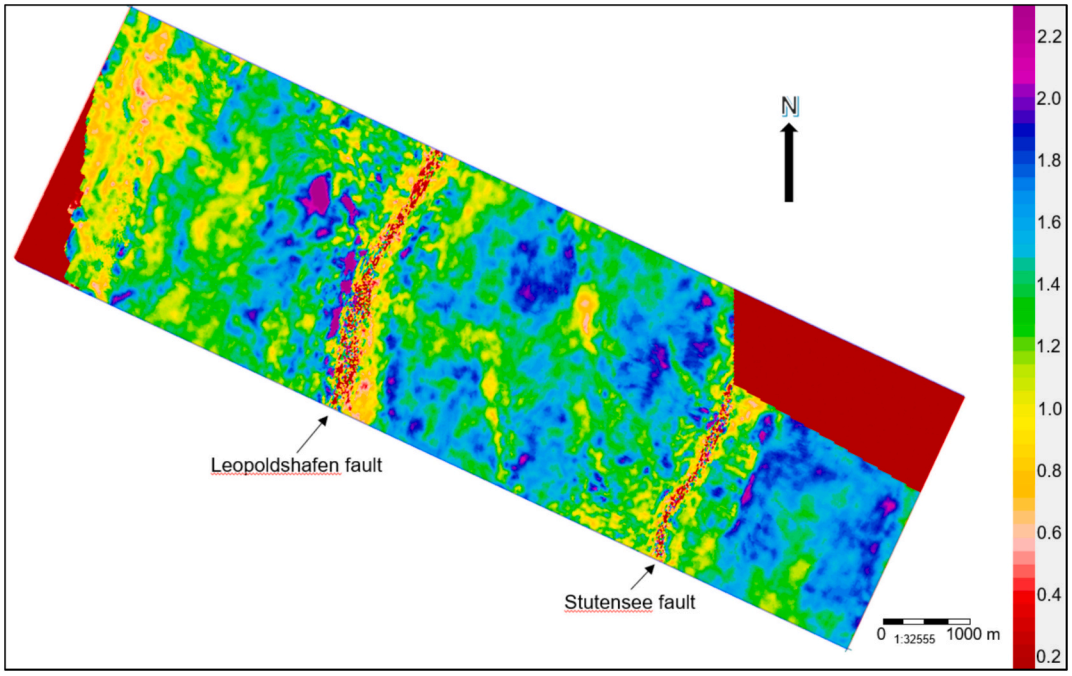

Fig. 6. RMS amplitude map for the Late Oligocene stratigraphy: spatial distribution of amplitude over the target interval, showing the main structure elements (Leoppldshafen & Stutensee) but without clear resolution of smaller-scale depositional features such as paleochannels.

scale features, such as fluvial channels, remain poorly resolved owing to the limitations of traditional seismic analysis techniques. This observation motivated the implementation of more advanced methodologies specifically tailored to enhance the detection and characterization of channel systems within the target interval.

3.3. *Spectral decomposition application*

Spectral decomposition is a technique that decomposes seismic data into its constituent frequency components, allowing for the isolation and enhancement of features that respond differently to various frequency bands. This approach is particularly effective for detecting thin beds and stratigraphic features below conventional resolution limits, making it

ideal for the identification of fluvial channel systems (El Kady et al., 2024). Fig. 7 illustrates a typical workflow for seismic spectral decomposition analysis, highlighting its sequential stages from the raw data interpretation to the extraction of frequency-dependent subsurface features. Initially, a 3D seismic volume in the time or depth domain is acquired, representing the full seismic dataset. This volume undergoes structural and stratigraphic interpretation, leading to an interpreted 3D seismic volume where key reflectors, horizons, and geological boundaries are delineated. Following interpretation, the data is subjected to spectral decomposition, a signal processing technique that transforms the seismic traces from the time or depth domain into the frequency domain, thereby isolating different frequency components associated with specific geological features. This results in frequency-based attribute volumes, which can reveal subtle stratigraphic features, discontinuities, or thin beds that are otherwise not visible in conventional seismic amplitudes. The final stage involves the integration of spectral attributes with geological and petrophysical data to enhance reservoir characterization and improve subsurface understanding. This workflow underscores the value of spectral decomposition in resolving geological complexities, particularly in stratigraphic and thin-bed analysis (Marfurt and Alves, 2015; Partyka et al., 1999).

To optimize the effectiveness of the spectral decomposition analysis, several preparatory steps were undertaken.

The seismic volume was spatially and temporally cropped using HampsonRussell to isolate the Late Oligocene target interval and exclude stratigraphically irrelevant overburden and underburden intervals. This data-cropping step reduced the computational burden for subsequent processing while ensuring that analyses remained focused on the interval of geological interest (Fig. 8). The cropped volume thus provides a clean dataset for high-resolution attribute generation, minimizing noise introduced by extraneous strata and improving the interpretability of subtle seismic anomalies. This approach is consistent with recommended practices for seismic geomorphological workflows, where proper cropping prior to time-frequency or spectral decomposition helps to reveal stratigraphic and structural features otherwise hidden in broadband data (Mandong and Saputra, 2025).

Horizon flattening was applied by selecting a key stratigraphic marker within the Late Oligocene succession and transforming the seismic volume such that all traces were shifted to align this surface horizontally (Fig. 9). This procedure removes the influence of post-depositional structural deformation—such as faulting, folding, or gentle tilting—thereby restoring the depositional geometry to its approximate paleo-horizontal state. As a result, time-equivalent sedimentary bodies appear on a common horizontal slice, greatly enhancing the visibility of lateral facies variations, including fluvial channels and associated geomorphological elements. Horizon flattening is widely recognized as a crucial step in seismic geomorphology, particularly when aiming to delineate subtle stratigraphic features obscured by structural overprints (Posamentier and Kolla, 2003).

A preliminary frequency analysis was performed prior to applying full spectral decomposition in order to determine the optimal frequency bands capable of resolving key geomorphological features within the Late Oligocene interval. This evaluation involved computing time–frequency gathers at strategically selected locations across the survey area, thereby enabling an assessment of the frequency-dependent seismic response of the flattened data (Fig. 10). By examining the spectral behavior along a representative seismic line, the analysis demonstrated how individual frequencies—such as the constant 26 Hz component—enhance specific reflectivity patterns associated with potential channel bodies. The resulting frequency-response characteristics guided through (Xline 615) the selection of an optimal RGB-blended frequencies set (10, 26, and 40 Hz), ensuring improved delineation of subtle stratigraphic elements during subsequent spectrum-decomposition processing. Such pre-analysis of frequency content is considered a best practice in seismic spectral decomposition workflows to maximize interpretational resolution (Castagna and Sun, 2006).

In this study, we implemented a short-time Fourier transform (STFT) algorithm to generate a series of frequency slices ranging from 10 to 50

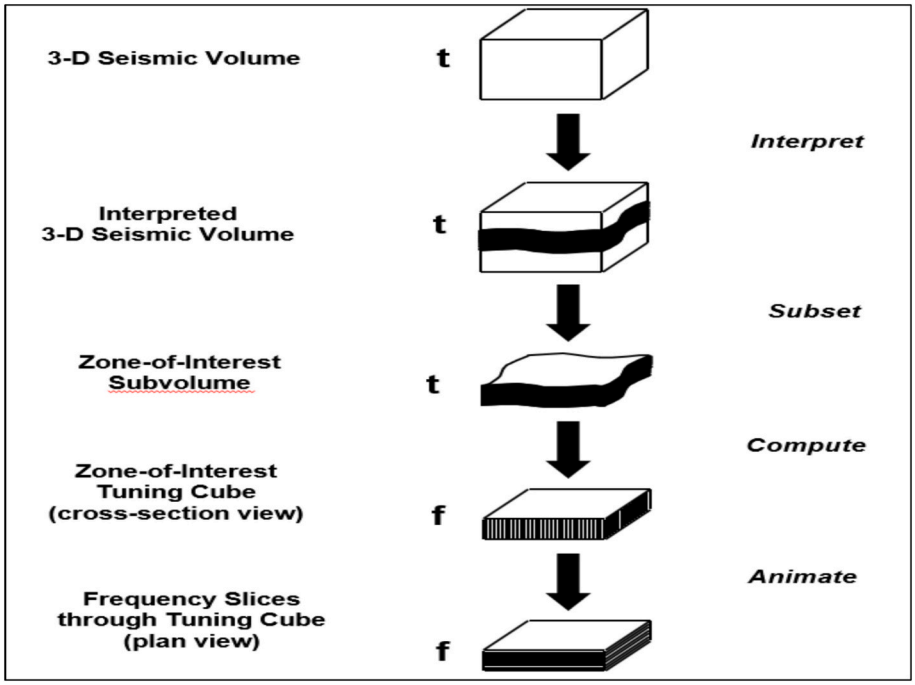

Fig. 7. Workflow for seismic spectral-decomposition analysis. The process begins with the full 3-D seismic volume, followed by structural and stratigraphic interpretation to define key horizons and intervals of interest. The interpreted volume is then spatially and temporally subsetted to extract a focused zone-of-interest subvolume. A tuning cube is subsequently computed for this interval, shown here in cross-sectional view. Finally, frequency slices are generated from the tuning cube in plan view, enabling visualization of depositional and geomorphological features as a function of frequency. This workflow forms the foundation for high-resolution spectral-decomposition–based stratigraphic analysis.(modified after Partyka et al., 1999).

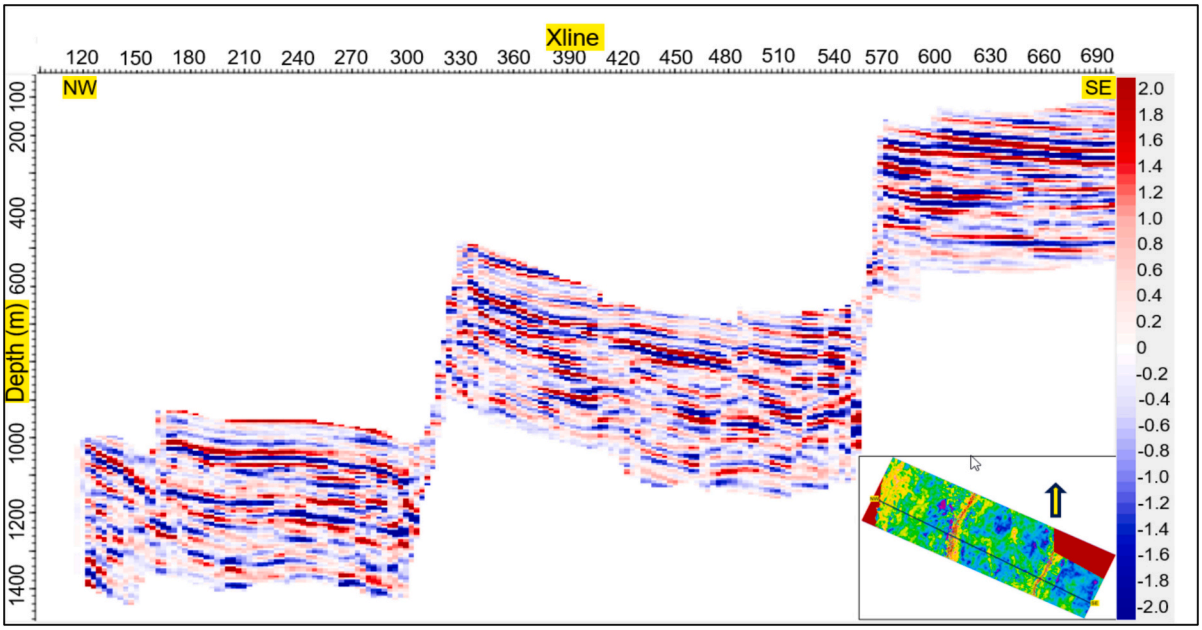

Fig. 8. Cropped seismic section restricted in depth and space to the Late Oligocene target zone, used for subsequent spectral decomposition and channel delineation.

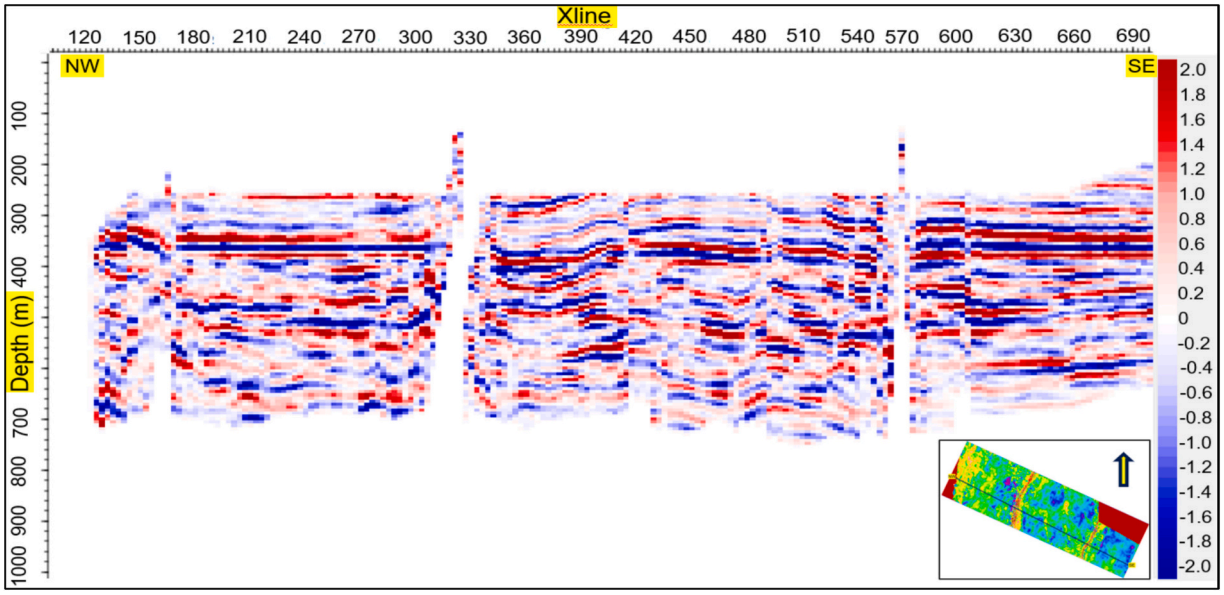

Fig. 9. Flattened seismic section flattened after aligning the reference Late Oligocene horizon, enabling clearer visualization of lateral stratigraphic features such as channel systems.

Hz at 2 Hz intervals. The STFT approach involves applying a Fourier transform to windowed segments of the seismic trace, effectively providing a time-frequency representation of the signal.

The Short-Time Fourier Transform (STFT) is a fundamental tool in signal processing for analyzing the frequency content of non-stationary signals over time. It extends the traditional Fourier Transform by incorporating a sliding window function, allowing the signal to be analyzed in both the time and frequency domains simultaneously. The STFT is mathematically defined as Eq. (1) (Partyka et al., 1999):

$$X_{STFT}[m,\omega] = \sum_{n=-\infty}^{\infty} x[n]\cdot w[n-m]\cdot e^{-i\omega n} \quad (1)$$

In this formulation, $x[n]$ is the discrete seismic trace, $w[n-m]$ is a localized window centered at sample m, and ω is the angular frequency. This transform enables a localized frequency analysis along the seismic trace, critical for detecting sub-resolution features such as thin fluvial channels. This transform provides a time-frequency representation that reveals how the spectral characteristics of the signal evolve, making it particularly useful for applications such as speech processing, audio analysis, and seismic data interpretation. In seismic studies, such as those exploring geothermal potential, STFT enables the identification of time-varying subsurface features by decomposing seismic signals into frequency components, facilitating the detection of geological structures like fluvial channels.

Based on the results of the frequency analysis in the time-frequency gather (Fig. 10), three key frequency components were selected for the RGB blended display: 10 Hz (assigned to red), 26 Hz (assigned to green), and 40 Hz (assigned to blue). This approach, following the methodology described by (Henderson et al., 2008), allows for the simultaneous

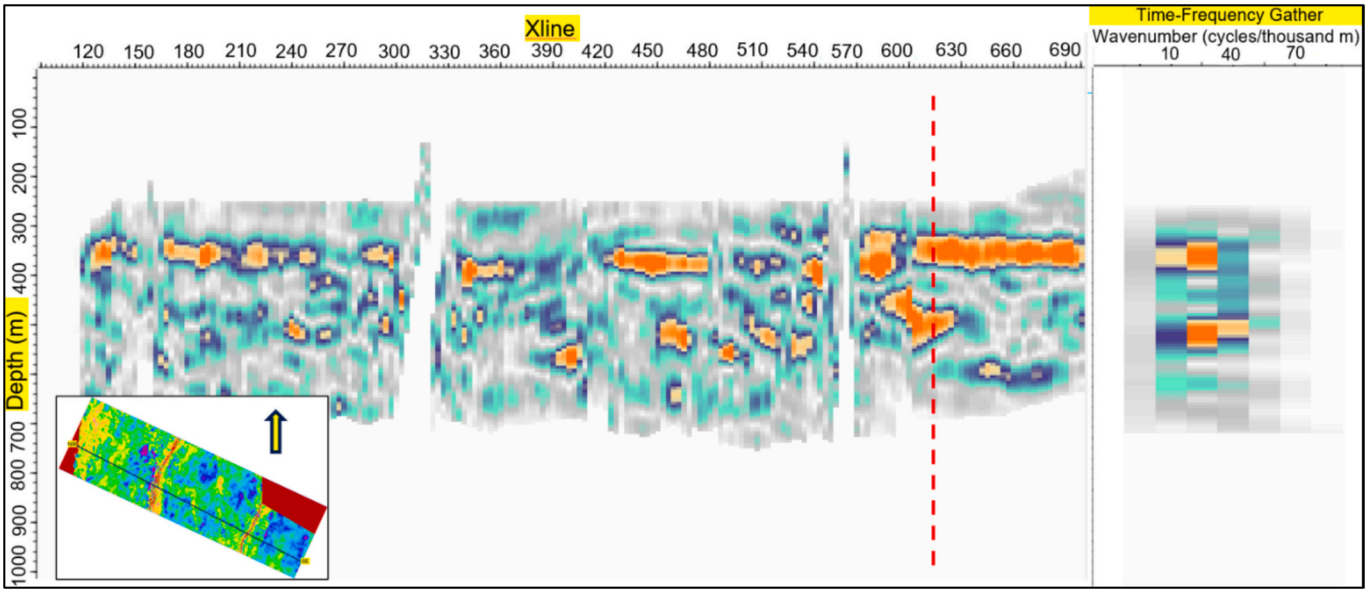

Fig. 10. Seismic section filtered at a constant 26 Hz to highlight frequency-dependent reflectivity and the corresponding frequency gather extracted along Xline 615 (dashed red line). This analysis was used to identify the optimal frequencies (10, 26, 40 Hz) for RGB spectral blending.

visualization of multiple frequency responses, with different geological features appearing as distinct color combinations based on their frequency-dependent characteristics.

Tuning analysis indicates that the dominant tuning frequency for the Late Oligocene sand-prone channel fills is approximately 26 Hz. This frequency corresponds to constructive interference of reflections from channel top and base interfaces and provides maximum amplitude response for beds with thicknesses close to the quarter-wavelength criterion. Consequently, 26 Hz was selected as the central tuning frequency for subsequent RGB spectral blending, supplemented by 10 Hz and 40 Hz to capture thicker and thinner stratigraphic elements, respectively

RGB blended displays were generated for a series of horizontal slices through the flattened seismic volume, providing a comprehensive view of the lateral variations in frequency response throughout the Late Oligocene interval. This approach was particularly effective in enhancing the visibility of channel features that were not discernible in conventional attribute displays.

4. Results

The application of spectral decomposition to the flattened seismic volume (Fig. 9) yielded remarkable improvements in the visualization of channel features within the Late Oligocene interval. The frequency analysis conducted through time-frequency gathers (Fig. 10) revealed distinct frequency responses for different geological elements, with channel features exhibiting particularly strong amplitude variations in the 10, 26, and 40 Hz components.

The RGB-blended spectral-decomposition volumes provided a significant enhancement in resolving geomorphological elements within the Late Oligocene interval (Fig. 11; Fig. 12). These composite displays illuminated a network of meandering channel systems expressed as continuous curvilinear features with distinctive color signatures that reflect their unique multi-frequency responses. The improved detectability arises from the differential tuning behavior of thin-bedded channel fills relative to the surrounding lithologies, allowing subtle variations in bed thickness and lithofacies to appear as contrasting RGB patterns. This constitutes the first unambiguous visualization of the channel architecture in the study area, demonstrating the effectiveness of spectral decomposition in delineating stratigraphic heterogeneities that remain unresolved in conventional seismic attributes.

The integration of observations from multiple horizontal slices

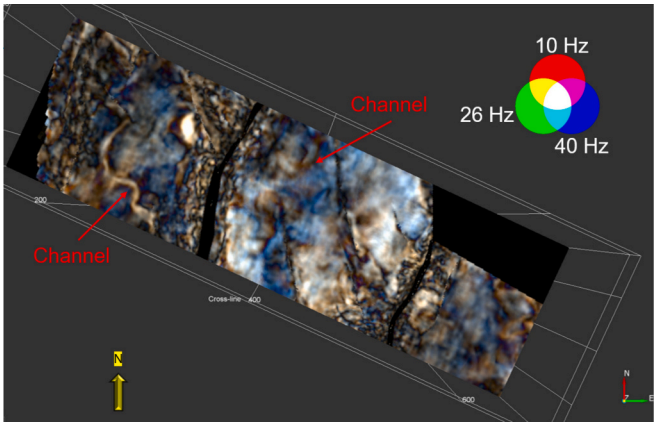

Fig. 11. Seismic spectral decomposition map of the upper section of the target zone, visualized using RGB blending of frequency components at 10 Hz (red), 26 Hz (green), and 40 Hz (blue). This representation enhances the delineation of stratigraphic and geomorphological features based on their frequency-dependent reflectivity. (For interpretation of the references to colour in this figure legend, the reader is referred to the web version of this article.)

through the flattened volume allowed the mapping of a pretty comprehensive channel network throughout the Late Oligocene interval (Fig. 13). In total, 25 distinct channel systems were identified and manually delineated within the study interval, exhibiting a predominant NE-SW orientation that likely reflects the regional topographic gradient during the Late Oligocene, with a minor NW-SE trending channel at the base of the layer. This channel's orientation may be associated with sediment transport from the uplifted graben shoulders toward the central axis of the URG.

The thickness of the mapped fluvial channel bodies was quantitatively estimated using the frequency-dependent seismic tuning relationship derived from spectral decomposition analysis. According to the thin-bed tuning model described by (Partyka et al., 1999). The maximum composite reflection amplitude occurs when bed thickness approaches one-quarter of the dominant seismic wavelength ($\lambda/4$). Under this condition, the vertical bed thickness (d) can be expressed in Eq. (2):

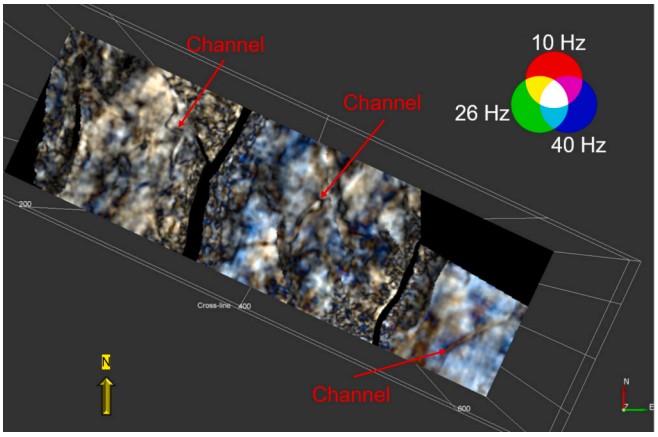

Fig. 12. Seismic spectral decomposition map of the middle section of the target zone, visualized using RGB blending of frequency components at 10 Hz (red), 26 Hz (green), andm 40 Hz (blue). This representation reveals additional channelized elements and stratigraphic variations not apparent in broadband or single-attribute seismic displays. (For interpretation of the references to colour in this figure legend, the reader is referred to the web version of this article.)

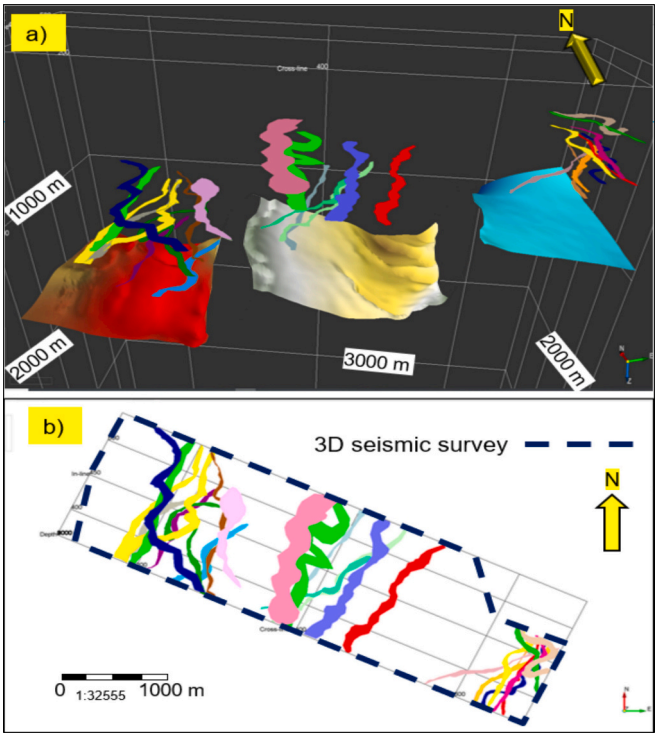

Fig. 13. Distribution of the Oligocene fluvial channels. (a) Three-dimensional visualization of the channel network integrated with the interpreted Fish Shale horizon. (b) Two-dimensional map view of the channels overlaid with the outline of the 3D seismic survey area, illustrating the spatial extent and orientation within the study region.

$$d = \frac{V}{4f} \tag{2}$$

where V denotes the average P-wave interval velocity, and f represents the dominant tuning frequency identified from the spectral amplitude response. For the investigated Late Oligocene siliciclastic succession, interval velocities are assumed to range between 2400 and 2500 m/s, consistent with regional geophysical velocity models for marly-mudstone and sandstone sequences. Spectral decomposition results indicate a dominant tuning frequency of approximately 26 Hz within the channel fairways. Substituting an average velocity of 2500 m/s into the tuning relationship yields an estimated channel thickness of approximately 24 m.

In addition, the presence of higher-frequency components (e.g., ~40 Hz) within the seismic bandwidth enhances the detectability of thinner stratigraphic units, implying a minimum resolvable thickness on the order of 15 m. Consequently, the integrated spectral analysis suggests that the mapped channel bodies exhibit thicknesses ranging from approximately 15 to 24 m. This thickness range is consistent with documented fluvial reservoir analogues in rift-related basin settings and further supports the geological plausibility and geothermal reservoir potential of the identified channel systems.

The channel network displays a hierarchical structure, with smaller tributary channels (25–40 m wide) feeding larger trunk channels (60–100 m wide). This organization suggests a well-developed drainage system with multiple orders of streams, which is typical of mature fluvial environments. The spatial distribution of channels was not uniform across the study area, with a higher density observed in the central and eastern blocks than in the western block. Stacking of channels and accumulation of >200 m fluviatile sediments indicate ongoing tectonic subsidence on the development of preferential-drainage pathways.

The identification of these channel systems represents a significant advancement in our understanding of the depositional history of the Upper Oligocene in Karlsruhe. The channels, previously undetectable through conventional seismic analysis, provide valuable insights into paleogeography and sediment dispersal patterns during this period in the evolution of the Upper Rhine Graben.

5. Discussion & conclusion

5.1. Channel systems in the oligocene depositional environments

The identification of at least 25 meandering channel systems provides insights into the distribution and geometry of sand-rich successions of the Niederrödern Fm. in the Upper Rhine Graben. These findings also corroborate the previously proposed fluvial depositional system detected in Niederrödern Fm. (Berger et al., 2005).

Although our survey is relatively small, it appears that channels developed from higher sinuosity and complex branching to lower sinuosity. This could indicate a slight increase in stream power due to changes in the base level, sediment supply, or tectonic activity. Drilling reports from the Niederrödern Fm. document calcite cemented (mostly fine, partly medium, grained) sandstones with permeabilities ranging from <1 mD to 108 mD and individual thicknesses of up to 30 m. A possible increase in stream power could have been associated with the onset of the development of the intra-rift Heidelberg Basin due to late Oligocene stress field change (for example Bauer et al., 2025; Grimmer et al., 2017).

The detailed characterization of channel systems achieved by spectral decomposition significantly enhances our understanding of the subsurface architecture of the Karlsruhe area. Prior to this study, the internal heterogeneity of the Late Oligocene interval was poorly constrained, with conventional seismic attributes providing only a general view of the stratigraphic framework. The newly identified channel network reveals a complex mosaic of potentially higher-permeability bodies embedded within a lower-permeability matrix, fundamentally altering our conceptualization of fluid flow pathways within this interval.

This improved understanding of subsurface heterogeneities has important implications for various applications, including hydrocarbon exploration and thermal energy storage. The spatial distribution and connectivity of channel systems directly influence fluid flow patterns, which in turn affect the heat transport mechanisms relevant to geothermal resource assessment. By mapping these preferential flow pathways with unprecedented detail, this study provides a foundation

for more accurate reservoir modeling and simulation efforts.

Comparable fluvial channel architectures have been documented in several successful geothermal provinces worldwide. In the Paris Basin, spectrally enhanced seismic interpretation revealed channelized sand bodies that act as primary geothermal reservoirs (Dezayes et al., 2009). Similar results were reported from the South German Molasse Basin, where fluvial sandstones with thicknesses of 10–30 m form laterally continuous geothermal targets (Przybycin et al., 2017). In the Netherlands, spectral decomposition has been successfully applied to delineate thin fluvial reservoirs within Rotliegend successions, significantly improving well targeting and productivity forecasts (Doornenbal and Stevenson, 2010). The channel dimensions and stacking patterns identified in the present study fall well within the range of these proven geothermal analogues, reinforcing their relevance for geothermal utilization in the Upper Rhine Graben.

Furthermore, the ability to detect channels as narrow as 25 m using advanced seismic analysis techniques represents a significant methodological advancement. This resolution enhancement pushes the boundaries of what is typically achievable with conventional 3D seismic data, opening new possibilities for detailed stratigraphic interpretation in similar geological settings worldwide. The workflow developed in this study, which combines horizon flattening with RGB blended spectral decomposition, provides a template that can be readily applied to other datasets facing similar resolution challenges.

5.2. Limitations and outlooks

While this study has significantly advanced our understanding of the depositional system of the Niederrödern Fm. in the Karlsruhe area, limitations and uncertainties must be addressed. First, no seismic channel was intersected by a well; hence, no petrophysical properties could be assigned to the channels within the study area. On the other hand, where borehole data are available, seismic imaging is reduced due to fault shadowing effects and partial faulting out of strata. This limitation introduces uncertainty regarding the exact composition and petrophysical properties of the identified channel fills, which could range from high-permeability sands to more heterolithic, lower-permeability deposits, as indicated by the range of permeability data.

Second, the resolution limitations of seismic data, even with advanced spectral decomposition techniques, mean that smaller-scale features, such as crevasse splays and minor tributary channels, are likely to remain undetected. These elements can significantly influence the overall connectivity of the channel network and should be considered to exist and contribute to fluid flow in conceptual models, despite their absence in seismic imaging and interpretation.

Expanding the study area to encompass a larger portion to the north of the study area would also provide valuable context for understanding the regional significance of the identified channel systems in the study area. By mapping the full extent of these depositional elements beyond the current 10 km × 4 km survey, a more comprehensive understanding of the development of the channel networks could be achieved.

Finally, the integration of the seismic interpretations with numerical modeling of fluid flow and heat transport would allow for a quantitative assessment of the impact of channel heterogeneity on geothermal resource potential. Such modeling efforts could provide valuable insights into the relative importance of different geological factors controlling thermal anomalies and guide future exploration and development strategies in the region.

CRediT authorship contribution statement

Amr Talaat Tolba: Writing – review & editing, Writing – original draft, Visualization, Validation, Software, Resources, Methodology, Formal analysis, Data curation, Conceptualization. **Florian Bauer:** Writing – review & editing, Validation, Supervision, Methodology. **Jens Carsten Grimmer:** Writing – review & editing, Validation, Supervision. **Ali Dashti:** Writing – review & editing. **Thomas Kohl:** Supervision.

Declaration of competing interest

The authors declare the following financial interests/personal relationships which may be considered as potential competing interests:

Amr Talaat Tolba reports financial support was provided by Helmholtz Association of German Research Centres. Amr Talaat Tolba reports a relationship with Karlsruhe Institute of Technology that includes: employment. If there are other authors, they declare that they have no known competing financial interests or personal relationships that could have appeared to influence the work reported in this paper.

Acknowledgments

The authors gratefully acknowledge Neptune Energy & Palatina GeoCon and Lime Resources for providing access to the high-resolution 3D seismic dataset that formed the basis of this research. We also thank the Helmholtz Association for funding support, which made this project possible. Additionally, we express our appreciation to Geosoftware for providing access to the HampsonRussell software, which was instrumental in the seismic analysis and interpretation carried out in this study. Open Access funding enabled and organized by Projekt DEAL.

Data availability

The data that has been used is confidential.

References

Acocella, V., 2005. Modes of sector collapse of volcanic cones: insights from analogue experiments. J. Geophys. Res. Solid Earth 110 (B2), 2004JB003166. https://doi.org/10.1029/2004JB003166.

Agemar, T., Schellschmidt, R., Schulz, R., 2012. Subsurface temperature distribution in Germany. Geothermics 44, 65–77. https://doi.org/10.1016/j.geothermics.2012.07.002.

Bauer, F., Grimmer, J.C., Houpt, L., Hertweck, T., Schill, E., 2025. Development of Intra-Rift Basins during stress field change in the Central Upper Rhine Graben (SW Germany). Tectonics 44 (4), e2024TC008721. https://doi.org/10.1029/2024TC008721.

Berger, J.-P., Reichenbacher, B., Becker, D., Grimm, M., Grimm, K., Picot, L., Storni, A., Pirkenseer, C., Schaefer, A., 2005. Eocene-Pliocene time scale and stratigraphy of the Upper Rhine Graben (URG) and the Swiss Molasse Basin (SMB). Int. J. Earth Sci. 94 (4), 711–731. https://doi.org/10.1007/s00531-005-0479-y.

Binder, T., Marks, M.A.W., Gerdes, A., Walter, B.F., Grimmer, J., Beranoaguirre, A., Wenzel, T., Markl, G., 2023. Two distinct age groups of melilitites, foidites, and basanites from the southern Central European Volcanic Province reflect lithospheric heterogeneity. Int. J. Earth Sci. 112 (3), 881–905. https://doi.org/10.1007/s00531-022-02278-y.

Böcker, J., Littke, R., Forster, A., 2017. An overview on source rocks and the petroleum system of the central Upper Rhine Graben. Int. J. Earth Sci. 106 (2), 707–742. https://doi.org/10.1007/s00531-016-1330-3.

Brown, A.R., 2011. Interpretation of three-dimensional seismic data. Am. Assoc. Petrol. Geolog. https://doi.org/10.1306/m4271346.

Castagna, J.P., Sun, S., 2006. Comparison of spectral decomposition methods. First Break 24 (3). https://doi.org/10.3997/1365-2397.24.1093.26885.

Derer, C.E., Schumacher, M.E., Schäfer, A., 2005. The northern Upper Rhine Graben: Basin geometry and early *syn*-rift tectono-sedimentary evolution. Int. J. Earth Sci. 94 (4), 640–656. https://doi.org/10.1007/s00531-005-0515-y.

Dezayes, C., Genter, A., Valley, B., 2009. Structure of the low permeable naturally fractured geothermal reservoir at Soultz. Comptes Rendus. Géosci. 342 (7–8), 517–530. https://doi.org/10.1016/j.crte.2009.10.002.

Doornenbal, H., Stevenson, A., 2010. Petroleum Geological Atlas of the Southern Permian Basin Area [Map]. TNO Geological Survey of the Netherlands.

El Kady, H., Talaat, A., Gad, K.H., 2024. Integrated seismic attributes as a tool to delineate the oligocene channels architecture, Baltim Field, Offshore Central Nile Delta, Egypt. Iraqi Geol. J. 139–151. https://doi.org/10.46717/igj.57.2C.11ms-2024-9-19.

Geyer, O.F., Gwinner, M.P., Geyer, M., Nitsch, E., Simon, T., 2011. Geologie von Baden-Württemberg (5., völlig neu bearbeitete Auflage). Schweizerbart.

Grimm, K.I., 2011. Tertiär. Schweizerbart.

Grimmer, J.C., Ritter, J.R.R., Eisbacher, G.H., Fielitz, W., 2017. The Late Variscan control on the location and asymmetry of the Upper Rhine Graben. Int. J. Earth Sci. 106 (3), 827–853. https://doi.org/10.1007/s00531-016-1336-x.

Henderson, J., Purves, S.J., Fisher, G., Leppard, C., 2008. Delineation of geological elements from RGB color blending of seismic attribute volumes. Lead. Edge 27 (3), 342–350. https://doi.org/10.1190/1.2896625.

Kolditz, O., Bauer, S., Bilke, L., Böttcher, N., Delfs, J.O., Fischer, T., Görke, U.J., Kalbacher, T., Kosakowski, G., McDermott, C.I., Park, C.H., Radu, F., Rink, K., Shao, H., Shao, H.B., Sun, F., Sun, Y.Y., Singh, A.K., Taron, J., Zehner, B., 2012. OpenGeoSys: an open-source initiative for numerical simulation of thermo-hydro-mechanical/chemical (THM/C) processes in porous media. Environ. Earth Sci. 67 (2), 589–599. https://doi.org/10.1007/s12665-012-1546-x.

Lala, A.M.S., Talaat, A., 2020. A new exploration tool for subtle stratigraphic traps in the offshore Nile Delta, Egypt. Pet. Geosci. 26 (3), 434–447. https://doi.org/10.1144/petgeo2018-164.

Mandong, A., Saputra, R., 2025. Advancing seismic interpretation through spectral decomposition: techniques, applications, and innovative visualization. EAGE Workshop Adv. Seismic Solut. Complex Reserv. Challeng. 1–5. https://doi.org/10.3997/2214-4609.202571004.

Marfurt, K.J., Alves, T.M., 2015. Pitfalls and limitations in seismic attribute interpretation of tectonic features. Interpretation 3 (1), SB5–SB15. https://doi.org/10.1190/int-2014-0122.1.

Naseer, M.T., 2026. Spectral decomposition-based temperature and water saturation-constrained dynamical simulations detect high-temperature geothermal energy resource. Renew. Energy 256, 123356. https://doi.org/10.1016/j.renene.2025.123356.

Ogola, P.F.A., Davidsdottir, B., Fridleifsson, I.B., 2012. Opportunities for adaptation-mitigation synergies in geothermal energy utilization - initial conceptual frameworks. Mitig. Adapt. Strateg. Glob. Chang. 17 (5), 507–536. https://doi.org/10.1007/s11027-011-9339-1.

Partyka, G., Gridley, J., Lopez, J., 1999. Interpretational applications of spectral decomposition in reservoir characterization. Lead. Edge 18 (3), 353–360. https://doi.org/10.1190/1.1438295.

Pirkenseer, C., Berger, J.-P., Reichenbacher, B., 2013. The position of the Rupelian/Chattian boundary in the southern Upper Rhine Graben based on new records of microfossils. Swiss J. Geosci. 106 (2), 291–301. https://doi.org/10.1007/s00015-013-0146-4.

Posamentier, H.W., Kolla, V., 2003. Seismic geomorphology and stratigraphy of depositional elements in deep-water settings. J. Sediment. Res. 73 (3), 367–388. https://doi.org/10.1306/111302730367.

Pribnow, D., Schellschmidt, R., 2000. Thermal tracking of upper crustal fluid flow in the Rhine Graben. Geophys. Res. Lett. 27 (13), 1957–1960. https://doi.org/10.1029/2000GL008494.

Przybycin, A.M., Scheck-Wenderoth, M., Schneider, M., 2017. The origin of deep geothermal anomalies in the German Molasse Basin: results from 3D numerical models of coupled fluid flow and heat transport. Geotherm. Energy 5 (1), 1. https://doi.org/10.1186/s40517-016-0059-3.

Reinhold, C., Schwarz, M., Perner, M., 2016. The Northern Upper Rhine Graben: Re-dawn of a Mature Petroleum Province? [Text/html,application/pdf,text/html] https://doi.org/10.5169/SEALS-658196.

Rotstein, Y., Schaming, M., Rousse, S., 2005. Structure and Tertiary tectonic history of the Mulhouse High, Upper Rhine Graben: block faulting modified by changes in the Alpine stress regime. Tectonics 24 (1), 2004TC001654. https://doi.org/10.1029/2004TC001654.

Stricker, K., Grimmer, J.C., Egert, R., Bremer, J., Korzani, M.G., Schill, E., Kohl, T., 2020. The potential of depleted oil reservoirs for high-temperature storage systems. Energies 13 (24), 6510. https://doi.org/10.3390/en13246510.

Von Eynatten, H., Kley, J., Dunkl, I., Hoffmann, V.-E., Simon, A., 2021. Late Cretaceous to Paleogene exhumation in central Europe – localized inversion vs. Large-scale domal uplift. Solid Earth 12 (4), 935–958. https://doi.org/10.5194/se-12-935-2021.

Wirth, E., 1962. Die Erdöllagerstätten Badens. In: Abhandlungen Des Geologischen Landesamtes Baden-Württemberg, Monographic Series by the Geological Survey of Baden-Württemberg, 4, pp. 63–80.

Zhang, J., Geng, Y., Li, Z., Li, P., Wang, T., Xu, G., Yu, K., Wang, W., Wang, P., Guo, M., 2025. Modeling sediment flux in river confluences: a comprehensive momentum-based study. Water Resour. Res. 61 (10), e2024WR039154. https://doi.org/10.1029/2024WR039154.

Zhao, Y., Yi, J., Yao, R., Li, F., Hill, R.L., Gerke, H.H., 2024. Dimensionality and scales of preferential flow in soils of Shale Hills hillslope simulated using HYDRUS. Vadose Zone J. 23 (4), e20367. https://doi.org/10.1002/vzj2.20367.